Physica D 433 (2022) 133194

Contents lists available at ScienceDirect

Physica D

journal homepage: www.elsevier.com/locate/physd

Pattern formation in a predator–prey system with a finite interaction range in a channel-like region using the Fick–Jacobs diffusion approach

Mayra Núñez-López [a,*], Guillermo Chacón-Acosta [b]

[a] Department of Mathematics, Instituto Tecnológico Autónomo de México Río Hondo 1, Col. Progreso Tizapán Ciudad de México, C.P. 01080, Mexico
[b] Applied Mathematics and Systems Department, Universidad Autónoma Metropolitana-Cuajimalpa, Vasco de Quiroga 4871, Ciudad de México C.P. 05348, Mexico

ARTICLE INFO

Article history:
Received 5 May 2021
Received in revised form 30 December 2021
Accepted 2 February 2022
Available online 12 February 2022
Communicated by J. Dawes

Keywords:
Predator–prey system
Turing patterns
Fick–Jacobs–Zwanzig operator
Confined diffusion

ABSTRACT

In this work, we present a diffusive predator–prey model with a finite interaction scale between species and an external flow. The system is confined to a two-dimensional domain with one coordinate larger than another, which allows us to use the one-dimensional projection of the diffusion operator, known as the Fick–Jacobs projection, here with an external force. Within this approach, we obtain analytical results for an exponential-shaped channel showing that patterns can emerge through the diffusion-driven instability mechanism. We show that the range of unstable modes where patterns can appear is modified by the species interaction's spatial scale and an effective advection term that includes external velocity and the shape parameter that characterizes the channel-like region.

1. Introduction

Population ecology deals with the increases, decreases, and fluctuations of populations. In this sense, Lotka–Volterra equations focus on studying predator–prey competing species relations, where spatial variation is necessary to understand complete ecological behavior. These displacements might occur due to diffusive mechanisms when the organisms are embedded in a substrate or caused by their own propagation [1]. Competition between individuals establishes mechanisms to control growth caused by limited common resources. In complex ecological systems, so-called public goods interactions appear when opposing interests in the involved species are present. One way to study them is by imposing spatial limits on the evolution of the population [2,3]. Spatial dynamics influences in inter-species cooperation according to various emerging patterns [4]. It has been shown that in a population of individuals that diffuse, reproduce and compete for resources, non-local competitive interactions play a fundamental role in the spatial organization of such population. The non-local interaction has been effectively modeled by an influence function and a convolution operation in the reactive term, which leads to pattern formation [5,6].

The spatial relations between involved individuals can influence the formation of patterns under certain circumstances and become important when describing their behavior, which has been modeled through reaction–diffusion equations. The formation of patterns can reproduce the evolution of systems such as bacterial colonies [7], the concentration of plankton [8], the development of vegetation [9] or the spatial distribution of prey and predators [10,11], etc. In the latter case, Lotka–Volterra kind systems have been shown to generate patterns with the Turing mechanism. Diffusion-driven instabilities in population dynamics have been studied thoroughly. For instance, Bartumeus et al. [12] showed that Turing instability might be produced by interference among predators, by constructing a ratio dependent functional response, using a DeAngelis modified model [13]. McGehee and Peacock-López [14] and McGehee et al. [15] use a modified Bazykin model [13], where an interference term between predators produces diffusion-driven instability. The instability also appears through quadratic interaction terms, adequately delimited by Verhulst type saturations [1], or in a type II Holling functional response [16]. On the other hand, there are several models where prey-taxis allows predators to search more actively for prey and can generate different spatial patterns from those formed in models without prey-taxis [17–19]. Prey-taxis tends to reduce the likelihood of pattern formation in spatial predator–prey systems or even annihilate the spatial patterns [20], but other kind of taxis may have the opposite effect on pattern formation [21]. Other works investigate pattern formation with cross-diffusion that gives rise to a wide variety of patterns [22]. Many experiments of interest to chemists where cross-diffusion effects can be significant demonstrate that relatively small values of cross-diffusion parameters can lead to spatio-temporal pattern formation as long as the kinetics are sufficiently non-linear [23,24].

* Corresponding author.
E-mail address: mayra.nunez@itam.mx (M. Núñez-López).

https://doi.org/10.1016/j.physd.2022.133194
0167-2789/

Another non-linear and non-local interaction terms between species are characterized by a spatial scale that controls the interaction between prey and predators. This model is proposed since predation depends on the probability of finding a prey, so an integral over the action area appears in the reactive term. This term considers the influence of prey movements on predator behavior [10,11]. Given this kind of nonlinear spatial dependent terms, it is natural to think that if there are spatial limitations, they will also influence the system's behavior.

The influence of the boundaries has been studied in different works. In [25,26], both confinement and other effects such as the growth of the domain where the process takes place can affect patterns. The effects of boundary conditions and the coupling of Turing systems can generate patterns not shown by the standard model. Indeed, growth may be a mechanism to increase the robustness of pattern formation. In [27], one of the boundaries represents the predators' trajectories and the survival probability of the prey changes depending on the boundary's shape. In Ref. [28] a numerical study of the spatial correlations between predators and prey was carried out, observing the response of prey to the presence and actions of a predator in a limited space. Therefore, the prey's escape is influenced not only by the predator's movement but also by the confinement, although a thorough analysis is needed. There are some predator–prey systems where organisms inhabit environments such as streams and rivers, where there is naturally a preferential direction associated with a constant flow that is fundamental for populations' behavior. These systems have been modeled mainly as one-dimensional [29]. However, as small perturbations in the flows put these populations at risk, it would be interesting to analyze how the boundaries' variation affects this flux.

This work presents a prey–predator model within an external flow in a two-dimensional physical space projected in one effective dimension through the Fick–Jacobs projection method [30]. Unlike other works, in this paper, we propose to analytically study the influence of both an external advective velocity and the geometric characteristics of the domain in the formation of patterns modeled with a reaction–diffusion system with a spatial interaction scale in the reactive terms. This approach had not previously been studied to the best of the authors' knowledge. The analytical results show that the range of unstable modes, where patterns can arise, is influenced by the interaction distance between species, the external velocity, and the shape parameter indicating channel geometry variations.

The structure of the paper is as follows: In Section 2, we present the dispersion relation of the prey–predator model with spatial interaction in one and two-dimensional physical spaces. In Section 3, we consider the projection method to one dimension of the prey–predator model by introducing the Fick–Jacobs–Zwanzig (FJZ) differential operator with a position-dependent and a constant diffusion coefficient, as well as an external force inducing a velocity in the longitudinal direction. In this section, we accomplished the stability analysis of the system. We chose a channel with an exponential profile to obtain analytical results and study the parameter space of this system through the corresponding dispersion relation. We found that the range of untestable modes, where the patterns can arise, is modified due to advective terms, both external and geometrical-induced. Finally, in Section 4, we discuss and summarize our results.

2. Prey–predator model with spatial interaction

Let us consider a model characterized by a couple of equations, one for the prey $N(x,t)$ and one for the predator $P(x,t)$. They describe diffusion in physical space and the strength of the interaction in the nonlinear term is a function of individuals' proximity [31]. These reaction–diffusion models with spatial's scale interaction have been widely applied to model competition of species coevolution in community ecology. We introduce two different interactions scales $L_1 \neq L_2$ because we consider different effective ranges of interaction (the region where prey and predators interact may have different relevance to predator growth and prey death). This has an important role in pattern formation [10,32]

$$\frac{\partial N(x,t)}{\partial t} = D_N \frac{\partial^2 N(x,t)}{\partial x^2} + rN(x,t) - \alpha N(x,t)\int_{x-L_1}^{x+L_1} P(s,t)ds, \tag{1}$$

$$\frac{\partial P(x,t)}{\partial t} = D_P \frac{\partial^2 P(x,t)}{\partial x^2} - mP(x,t) + \beta P(x,t)\int_{x-L_2}^{x+L_2} N(s,t)ds \tag{2}$$

Predators consume the preys with an intrinsic rate α and reproduce with rate β, r is the preys' growth rate, and predators are assumed to die with rate m spontaneously. D_N and D_P are the constant diffusion coefficients of prey and predators, respectively.

The one-dimensional case was deeply analyzed in [10] to investigate the existence of patterns with spatial structure considering small harmonic perturbations for preys and predators, $A_N\, e^{\lambda t+ikx}$, $A_P\, e^{\lambda t+ikx}$ respectively. According to [10], the dispersion relation is given by

$$\widehat{\lambda}(K) = -K^2 + \frac{\sqrt{rm}L_1^2}{DK}\sqrt{-\sin^2 K\cos K}. \tag{3}$$

where $D_N = D_P = D$, $L_2 = 2L_1$, $K = kL_1$ and $\widehat{\lambda} = \lambda\frac{L_1^2}{D}$.

In [11] present some results related to the two-dimensional physical space with small harmonic perturbations $A_N \exp[\lambda t + i\bar{k}\cdot\bar{x}]$, $A_P \exp[\lambda t + i\bar{k}\cdot\bar{x}]$, where $\bar{x} = (x,y)$, and $\bar{k} = (k_x, k_y)$ is a two-dimensional wave vector of modulus $|\bar{k}| = k$, the dispersion relation is given by

$$\widehat{\lambda}(K) = -K^2 + \frac{\sqrt{rm}R^2}{DK}\sqrt{-J_1(K)J_1(2K)} \tag{4}$$

where J_1 is the first-order Bessel function, $D_N = D_P = D$, $R_1 = 2R_2 = 2R$, $K = kR$, $\widehat{\lambda} = \lambda\frac{R^2}{D}$. In both dispersion relationships the objective is to found for some K where $Re[\widehat{\lambda}(K)] > 0$ so spatial patterns can emerge i.e. is possible to record spatial correlations between prey and predators in nature. The presence of structures persists independently of the space dimension where the model can be implemented. For instance, in Ref. [11] it was shown that for a dimension greater than two, a larger difference between effective ranges of interaction promotes cluster formation.

Lotka–Volterra model characterized by a finite range prey–predator interaction in a two-dimensional space is the most appropriate for describing real ecosystems. The 3D case is not typical to model an ecosystem. Terrestrial individuals and even marine species tend to remain within a small thickness layer compared to their horizontal movements [11].

In the next section, we consider the projection of this model to one effective dimension of the prey–predator model.

3. Projection to one effective dimension

Let us consider a reaction–diffusion–advection model for the prey's $N(x,y,t)$ and predator's $P(x,y,t)$ densities, which can move in two-dimensional space [11]. Here we consider isotropic and constant diffusion coefficients, different for each species, i.e,

$D_{N_x} \neq D_{N_y} \neq D_{P_x} \neq D_{P_y}$, and an advective flow in the longitudinal direction with velocity v,

$$\frac{\partial N}{\partial t} = D_{N_x}\frac{\partial^2 N}{\partial x^2} + D_{N_y}\frac{\partial^2 N}{\partial y^2} + v\frac{\partial N}{\partial x} + rN - \alpha N \iint_{|\mathbf{x}'-\mathbf{x}|\in\Omega_1} P(x', y', t)dx'dy', \tag{5}$$

$$\frac{\partial P}{\partial t} = D_{P_x}\frac{\partial^2 P}{\partial x^2} + D_{P_y}\frac{\partial^2 P}{\partial y^2} + v\frac{\partial P}{\partial x} - mP + \beta P \iint_{|\mathbf{x}'-\mathbf{x}|\in\Omega_2} N(x', y', t)dx'dy', \tag{6}$$

where constant rates are as in Eqs. (1), (2), and $\mathbf{x} = (x, y)$, $|\mathbf{x}' - \mathbf{x}|$ is the distance calculated with the Euclidean norm, and Ω_1, Ω_2 are the action regions of the corresponding predator or prey, such that the integrals count the number of prey or predators with which they can interact. Usually, one considers fixed radius neighborhoods. Instead, we consider that the two-dimensional region where the entire process occurs is like a channel, i.e., one of the directions is much larger than the other so that the diffusion in the transverse direction will relax much faster than in the longitudinal direction, which will allow the use of an effective equation along the longitudinal coordinate. To carry out this procedure, it is necessary to project Eqs. (5) and (6) on the longitudinal coordinate x by integrating on the transverse coordinate y. Let us first introduce the marginal densities

$$n(x) = \int_{h_1(x)}^{h_2(x)} N(x, y, t)dy, \tag{7}$$

$$p(x) = \int_{h_1(x)}^{h_2(x)} P(x, y, t)dy, \tag{8}$$

where $h_1(x)$ and $h_2(x)$ are the channel-like region's upper and lower boundaries, which depend on the longitudinal coordinate. In Eqs. (5) and (6), the time derivative on the left-hand side and the fourth term on the right-hand side can be integrated directly. In the particular case with no advection, i.e. $v = 0$, we apply the fundamental theorem of calculus and Leibniz's rule to introduce the marginal densities for the terms with derivatives on the right-hand side of Eqs. (5) and (6). Furthermore, we must impose zero flux conditions at the transverse boundaries. These conditions make it possible to relate both the derivatives and the diffusion coefficients in different directions [33,34]. Under these assumptions, it is possible to rewrite the second-order derivatives on the right-hand side of (5) and (6), which correspond to the Laplacian operator, as the so-called Fick–Jacobs operator, which is as follows

$$\hat{L}_{FJ}(\cdot) = D_i\frac{\partial}{\partial x}\left[w(x)\frac{\partial}{\partial x}\left(\frac{\cdot}{w}\right)\right], \tag{9}$$

where $w(x) := h_2(x) - h_1(x)$ is the width function. Since Zwanzig's original work [34], it has been proposed that the diffusion coefficient in this approach may depend on the longitudinal coordinate [35]. The Kalinay and Percus projection method [36,37] provides a systematic way of finding position-dependent corrections of the diffusion coefficient. In this method, a perturbation series that consists of operators acting on the density is proposed. The diffusivity ratio is the perturbation parameter, i.e., it is assumed that the transverse diffusion is faster than the longitudinal one. This assumption is made because, as the transverse distance is much shorter, the particles will travel more frequently in that direction, facilitating the faster equilibration of that component. However, the ratio value is not a strict requirement since the series has been seen to converge even if the ratio is one [33,36,37]. On the other hand, employing differential geometry methods to parameterize the channel's shape, more general coefficients that depend on the midline's coordinate have also been found [38,39]. Therefore, the operator in (9) can be extended as follows,

$$\hat{L}_{FJZ_i}(\cdot) = \frac{\partial}{\partial x}\left[D_i(x)w(x)\frac{\partial}{\partial x}\left(\frac{\cdot}{w}\right)\right]. \tag{10}$$

with $D_i(x)$ the position dependent diffusion coefficient of the ith species.

Indeed, the dependence of the effective diffusion coefficient on x is specifically through $w'(x)$, and since Zwanwig [34], the channel width is asked to be slowly varying functions of x. Nevertheless, the validity range of this approximation has been explored in several works, both from an analytical and a numerical perspective [40–43]. They show that the constraint $w' \ll 1$ can be weakened to $w' \leq 1$, [43]. This approach has also been extended when additional effects such as hydrodynamic terms [44,45] or external fields causing advective currents [46,47], and even if the diffusion takes place on a curved surface [48]. Reactive terms have also been considered, [49]. Moreover, in Ref. [30] patterns formation in systems with reactive terms that occur in channel-like geometries was studied, obtaining that the Turing instability conditions are modified due to the channel's geometry. Also, in Ref. [30], it is seen that the effect of $D(x)$ can be absorbed in a rescaling of the longitudinal coordinate.

In the case of external fields it has been shown that, projecting the corresponding Smoluchowski equation, the lowest order in the method corresponds to the Fick–Jacobs equation with the operator (9), but with a width function modified by the corresponding external potential $U(x, y)$, as follows

$$\hat{L}_{FJA}(\cdot) = D_i\frac{\partial}{\partial x}\left[A(x)\frac{\partial}{\partial x}\left(\frac{\cdot}{A}\right)\right], \tag{11}$$

where

$$A(x) = \int_{h_1(x)}^{h_2(x)} e^{-\beta U(x,y)}dy, \tag{12}$$

with $\beta = 1/kT$. For higher orders, the Kalinay and Percus method leads to a x dependent diffusion coefficient that is a function of both the derivatives of the width function and complicated combinations of the external potential [46,47]. It is not difficult to see that the potential $U(x) = vx/D_i\beta$ produces an advective flow in the longitudinal direction with constant velocity v, which is just what is required for the analysis of the system (5)–(6). In such a case, the generalized width can be written as $A(x) = w(x)\exp\left[-\frac{vx}{D_i}\right]$. The ratio between the advection velocity and the diffusion coefficient works as a decrease rate of the width function.

In addition to all the previous considerations, we must make additional assumptions to deal with the nonlinear terms that contain the integrals in (5) and (6). Let us first consider the case in which the regions Ω_i are rectangles with a fixed base length L_i, with $i = 1, 2$. but whose heights can extend to the channel-like region's boundaries therefore vary as one advances in the longitudinal direction, i.e. $h_1(x) \leq y' \leq h_2(x)$. Therefore, the integrals over y' in (5)–(6) immediately give the marginal densities. Hence, the system becomes as follows

$$\frac{\partial n}{\partial t} = \hat{L}_{FJA_n}(n) + rn - \alpha n\int_{x-L_1}^{x+L_1} p(x', t)dx', \tag{13}$$

$$\frac{\partial p}{\partial t} = \hat{L}_{FJA_p}(p) - mp + \beta p\int_{x-L_2}^{x+L_2} n(x', t)dx', \tag{14}$$

for constant diffusion coefficients. The system (13)–(14) is very similar to the one-dimensional system studied in Ref. [10], but with the Fick–Jacobs operator with external force, instead of just the second derivative.

Now, let us consider the system (13)–(14), but written as follows

$$\frac{\partial n}{\partial t} = D_N \frac{\partial^2 n}{\partial x^2} - D_N\, n\, \frac{\partial^2 \ln A}{\partial x^2} - D_N \frac{\partial \ln A}{\partial x}\frac{\partial n}{\partial x} + rn - \alpha n \int_{x-L_1}^{x+L_1} p(x',t)dx', \tag{15}$$

$$\frac{\partial p}{\partial t} = D_P \frac{\partial^2 p}{\partial x^2} - D_P\, p\, \frac{\partial^2 \ln A}{\partial x^2} - D_P \frac{\partial \ln A}{\partial x}\frac{\partial p}{\partial x} - mp + \beta p \int_{x-L_2}^{x+L_2} n(x',t)dx', \tag{16}$$

where the Fick–Jacobs operator with external potential was expanded in terms of A. The relation between derivatives of the generalized and genuine width functions is straightforward

$$\frac{\partial \ln A}{\partial x} = \frac{\partial \ln w}{\partial x} - \frac{v}{D_i}, \qquad \frac{\partial^2 \ln A}{\partial x^2} = \frac{\partial^2 \ln w}{\partial x^2}. \tag{17}$$

It is worth mentioning that the right hand side of Eq. (17) is the balance between the entropic and the external forces. The stationary case is identical to the one-dimensional case [10] since the entropic potential couples only to the diffusive term, which vanishes in such case. Therefore $\bar{n} = \frac{m}{2\beta L_2}$, and $\bar{p} = \frac{r}{2\alpha L_1}$. Then we consider small perturbations around the stationary state as follows

$$n(x,t) = \bar{n} + a_n\, e^{\lambda t} u(x), \qquad p(x,t) = \bar{p} + a_p\, e^{\lambda t} u(x), \tag{18}$$

where we consider the exponential behavior in time at rate λ, to perform the stability analysis, and $u(x)$ for the spatial perturbation term. By substituting the perturbed solution in Eqs. (15)–(16), the reactive part of the equations is reduced to the one-dimensional case by keeping only the terms linear in the perturbation. However, there are terms induced by the entropic potential that must be analyzed. As already mentioned, Fick–Jacobs approximation is valid as long as the channel's shape varies slowly, i.e., $w' \ll 1$. We observe that the term of the second derivative is of a higher order because it includes terms w'' and $(w')^2$, so we can neglect that term. With this Eqs. (15)–(16) reduce to

$$\lambda a_n u = D_N a_n \frac{\partial^2 u}{\partial x^2} - D_N a_n \frac{\partial \ln A}{\partial x}\frac{\partial u}{\partial x} - \alpha \bar{n} a_p \int_{x-L_1}^{x+L_1} u(x')dx', \tag{19}$$

$$\lambda a_p u = D_P a_p \frac{\partial^2 u}{\partial x^2} - D_P a_p \frac{\partial \ln A}{\partial x}\frac{\partial u}{\partial x} + \beta \bar{p} a_n \int_{x-L_2}^{x+L_2} u(x')dx', \tag{20}$$

Usually, one considers a harmonic perturbation $u(x) = e^{ikx}$, that solves the Helmholtz equation. Nevertheless, for channels, the boundary's geometry modifies the equation, and the eigenfunctions of the modified operator are needed [30]. The problem with this method is the nonlinear integral term in Eqs. (15)–(16) which is not necessarily proportional to the function $u(x)$, and the stability analysis may become involved. Instead, we make the stability analysis in Fourier space by transforming Eqs. (19) and (20). Therefore, the transform is as follows

$$\lambda a_n \hat{u} = -k^2 a_n D_N \hat{u} - \frac{D_N}{2\pi} a_n \hat{f} * \hat{g} - \alpha \bar{n} a_p \frac{2\sin kL_1}{k}\hat{u}, \tag{21}$$

$$\lambda a_p \hat{u} = -k^2 a_p D_P \hat{u} - \frac{D_P}{2\pi} a_p \hat{f} * \hat{g} + \beta \bar{p} a_n \frac{2\sin kL_2}{k}\hat{u}, \tag{22}$$

where the $\hat{u}$ is the Fourier transform of u and the convolution is given by

$$\hat{f} * \hat{g} = \int \hat{f}(k-k')\hat{g}(k')dk', \tag{23}$$

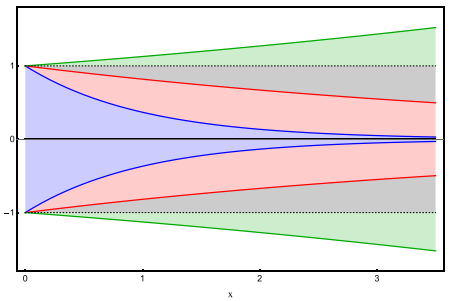

Fig. 1. Exponential funnel-like channel with different values for the shape parameter: $\gamma_0 = 1$ (blue), $\gamma_0 = 0.2$ (red), $\gamma_0 = 0$ (black dotted), $\gamma_0 = -0.12$ (green).

with

$$\hat{f} = \frac{1}{\sqrt{2\pi}} \int e^{-ikx} \frac{\partial \ln A}{\partial x} dx, \tag{24}$$

$$\hat{g} = \frac{1}{\sqrt{2\pi}} \int e^{-ikx} \frac{\partial u}{\partial x} dx = ik\hat{u}. \tag{25}$$

We see that Eqs. (21) and (22) are modified with respect to case 1D in Ref. [10] by the term that involves the Fourier transform of the generalized entropic potential.

In order to obtain analytical expressions for convolution in Eq. (23) we choose a channel with an exponential profile that has a funnel shape and whose width function is $w(x) = A_0\, e^{-\gamma_0 x}$. We can see a plot of this channel in Fig. 1. From Eq. (17), it can be seen that the kernel of $\hat{f}$, for this channel is a constant

$$\frac{\partial \ln A}{\partial x} = \frac{\partial}{\partial x} \ln\left(A_0 e^{-\gamma_0 x}\right) - \frac{v}{D_i} = -\gamma_0 - \frac{v}{D_i} \equiv -\gamma. \tag{26}$$

The Fourier transform of the derivative of the generalized entropic potential for this channel is $\hat{f} = -i\gamma\sqrt{2\pi}\delta(k)$. So, from (25) the convolution reduces to $\hat{f} * (ik\hat{u}) = \sqrt{2\pi}\gamma k\hat{u}$. For other width functions, for example, for periodic functions, either the convolution might not be proportional to $\hat{u}$, or the integral in (23) would have to be obtained numerically; this will be done elsewhere. Since our goal is to analytically study the effects of the interaction scale, advective flow, and channel geometry, we limit ourselves to studying the funnel-shaped channel. Further effects of periodic channels in reaction–diffusion systems with constant reaction rates have already been studied within the Fick–Jacobs approximation in [50].

3.1. Range of unstable modes of the dispersion relation

The system for stability analysis for this channel is

$$\left(\lambda + k^2 D_N + kD_N\gamma\right) a_n + \frac{m\alpha}{\beta}\frac{2\sin kL_1}{kL_2} a_p = 0, \tag{27}$$

$$\left(\lambda + k^2 D_P + kD_P\gamma\right) a_p - \frac{r\beta}{\alpha}\frac{2\sin kL_2}{kL_1} a_n = 0. \tag{28}$$

The characteristic polynomial is calculated when the determinant of the system equals zero, and is given by

$$\lambda^2 + (D_N + D_P)(k^2 + \gamma k)\lambda + h(k) = 0. \tag{29}$$

where

$$h(k) = D_N D_P k^4 + 2\gamma D_N D_P k^3 + \gamma^2 D_N D_P k^2 + \frac{rm}{k^2 L_1 L_2}\sin(kL_1)\sin(kL_2) \tag{30}$$

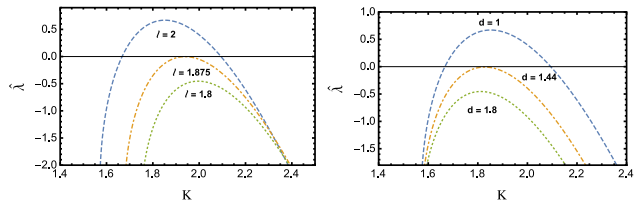

(a) (b)

Fig. 2. Dispersion relation $\widehat{\lambda}(K)$ for prey–predator model for $\Gamma = 0$ and $\mu = 15$ arbitrarily fixed. (a) Corresponds to $d = 1$ and $\ell = 2, 1.875, 1.8$. (b) For the values $\ell = 2$ and $d = 1, 1.44, 1.8$.

The corresponding solution to (29) is

$$\lambda = \frac{1}{2}(-(D_N + D_P)(k^2 + \gamma k)) \pm \frac{1}{2}\left[(D_N + D_P)^2(k^2 + \gamma k)^2 - 4\left(D_N D_P\left(k^4 + 2\gamma k^3 + \gamma^2 k^2\right) + \frac{rm\sin(kL_1)\sin(kL_2)}{k^2 L_1 L_2}\right)\right]^{1/2} \quad (31)$$

We can notice some things from Eq. (31). First, it is symmetric before exchanging the diffusion coefficients and the interaction lengths of predators and prey, respectively. Second, when $\gamma = 0$, the $\lambda(k)$ reduces to Eq. (3), therefore the condition $L_1 \neq L_2$ is at least necessary to guarantee pattern formation, as in [10]. The condition of vanishing γ can be obtained if both the shape factor and the current velocity are zero, or if $v = -D_i\gamma_0$; this will be discussed later.

By introducing the rescaled quantities $\widehat{\lambda} = \lambda\frac{L_1^2}{D_N}$, $K = kL_1$, $\mu = \sqrt{rm}L_1^2/D_N$, $\Gamma = L_1\gamma$, $d = D_P/D_N$, $\ell = L_2/L_1$, then the dispersion relation (31) becomes

$$\widehat{\lambda} = -\frac{(1+d)}{2}(K^2 + \Gamma K) \pm \frac{1}{2}\left[(1-d)^2(K^2 + \Gamma K)^2 - 4\mu^2\frac{\sin(K)\sin(K\ell)}{K^2\ell}\right]^{1/2}, \quad (32)$$

where prey quantities were chosen arbitrarily for the dimensionless variables due to the symmetry as said earlier.

Since we want to study the effects of advection and the influence of the channel geometry, we leave the case $\Gamma \neq 0$ for later and start with $\Gamma = 0$. In Fig. 2, plots of Eq. (32) are shown for $\Gamma = 0$ and $\mu = 15$. The latter value was chosen as a typical one to visualize the behavior of the dispersion relation as a function of the other parameters. The first plot is for variable d with $\ell = 2$ (a), and the other for variable ℓ with $d = 1$ (b). It can be seen that when ℓ increases, the length of unstable modes range also, but when ℓ tends to 1, the size of the range decreases. Indeed, there is no mode range for values smaller than $\ell_c \approx 1.875$, so patterns cannot be formed. On the other hand, for $d < 1$, the size of the range of modes increases, while if d increases, the range of modes decreases until $d_c \approx 1.44$, where there is only one mode that could form patterns. It is worth mentioning that in [10], numerical evidence was observed that $d = 1$ must be fulfilled. Therefore, for the following analysis we choose $d = 1$ and $\ell = 2$, with $\Gamma \neq 0$. Numerical experiments in this latter case are far from the scope of this work but will be done elsewhere.

With this choice for the parameters, the dispersion relation (32) simplifies to

$$\widehat{\lambda}(K) = -K^2 - \Gamma K + \mu\sqrt{-\frac{\sin K \sin 2K}{2K^2}}. \quad (33)$$

We require $\mathrm{Re}[\widehat{\lambda}(K)] > 0$ to find the limit from which spatial patterns emerge, i.e., the domain regions where the steady-state is unstable to spatial perturbations. The dispersion relation (33)

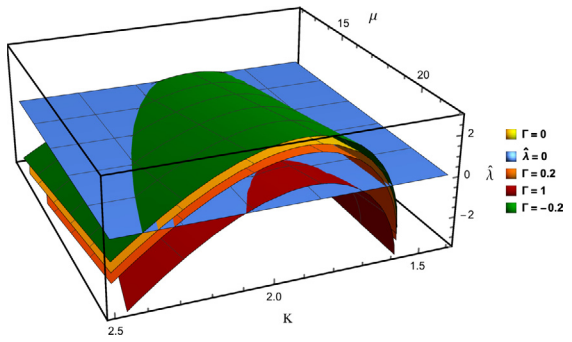

Fig. 3. Dispersion relation $\widehat{\lambda}(K)$ for exponential channel, plotted for different values of μ and Γ. The plane (blue) is the case $\widehat{\lambda} = 0$, the yellow surface is when $\Gamma = 0$. The red and orange surfaces are the cases for positive value of the parameter $\Gamma = 1$, 0.2, respectively; and the green is the negative case for $\Gamma = -0.2$.

differs from the 1D case [10], only by Γ, so the range of unstable modes now depends on both Γ and μ. In Fig. 3, the dispersion relation (33) is shown as a function of Γ and μ, where we can see that there will be μ values for which some Γ will prevent the formation of patterns in this system. Also, note that since Γ is a scaled quantity, its values also depend on action region length L_1, i.e., by varying this length, patterns can begin to form in the system.

The range of unstable wavenumbers is determined by the roots of Eq. (33) when the function $\hat{\lambda}$ has two real roots. This occurs according to the values of the parameters Γ and μ, since there could be two imaginary roots or a single point. Indeed, the case of a single point indicates the minimum value of the parameters for which the patterns start to emerge. The conditions to find this point and guarantee that it is a maximum are the following

$$\widehat{\lambda}(K) = 0, \quad (34)$$

$$\frac{\partial\widehat{\lambda}(K)}{\partial K} = 0, \quad (35)$$

$$\frac{\partial^2\widehat{\lambda}(K)}{\partial K^2} < 0. \quad (36)$$

The first two conditions can be seen geometrically as restrictions on the function (33), which form a system of equations whose solutions give the values of the parameters Γ, μ, as a function of K, and are the following

$$\mu(K) = -\frac{4K^4\csc(K)\sqrt{-\frac{\sin^2(K)\cos K}{K^2}}}{K - 4\sin(2K) + 3K\cos(2K)}, \quad (37)$$

$$\Gamma(K) = K\left(\frac{1}{-\frac{1}{2}K\tan K + K\cot K - 2} - 1\right). \quad (38)$$

These can be seen as the parametric equations of a curve $\mathcal{C}$ in the parameter space (K, Γ, μ).

On the other hand, we calculate the second derivative (36) to study the threshold value when it is equal to zero, from which it becomes negative, which indicates the presence of a maximum. From (33), we observe that the second derivative does not contain the parameter Γ, so it is possible to substitute $\mu(K)$ in it and find a threshold value K_m. This leads to the following expression

$$4K^4\sqrt{-\frac{\sin^2 K\cos K}{K^2}}\left(\frac{\csc K}{K - 4\sin(2K) + 3K\cos(2K)} + \Delta\right) = 0.$$

where

$$\Delta = \frac{4\cot K}{\sin K\left(11K^2 + \left(9K^2 - 8\right)\cos(2K) - 8\right) + 10K\cos K + 6K\cos(3K)}.$$

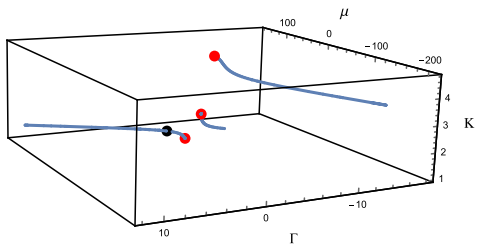

Fig. 4. Parametric plot of the dispersion relation (33) as a function of the wavenumber and the parameters μ and Γ. We plot for the values $1 \leq K \leq 5$, $-200 \leq \mu \leq 100$ and $-18 \leq \Gamma \leq 10$.

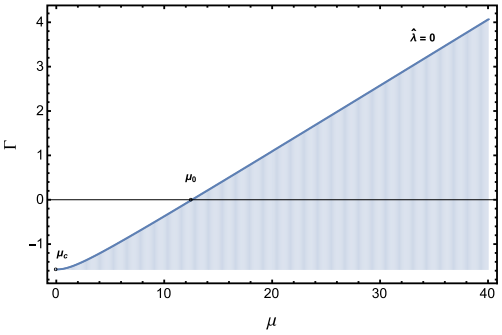

Fig. 5. Curve projection $\mathcal{C}$ on a plane as a function of μ and Γ. The shaded region indicates the patterns formation area (below the curve).

The real part of this equation has several real roots and also has some divergences. We show the first three roots (red dots) in Fig. 4. We see that each one corresponds to a different branch of the parametric curve. The root $K_1 = 4.7123$ corresponds to the values $\Gamma_1 = -4.712$ and $\mu_1 = -6.01954$, while $K_2 = 2.52715$ has $\Gamma_2 = -3.0655$ and $\mu_2 = -6.6032$.

A common feature of these points is that they have negative Γ and μ values. The parameter Γ can have negative values, indicating a competition between the two advection sources: the velocity v and the shape factor γ_0. However, according to the definition of μ through scaling, we note that it is a positive parameter, so we can choose as the critical value $\mu_c = 0$, which precisely corresponds to the root $K_c = 1.570796$, $\Gamma_c = -1.570796$, corresponding to the red dot in left branch shown in Fig. 4. If we return to the initial units, we have

$$k_c \approx \frac{1.570796}{L_1}, \qquad \gamma_c \approx \frac{-1.570796}{L_1}.$$

To obtain a numerical relation between μ and Γ, we can project the curve $\mathcal{C}$ on a plane regardless of its dependence on K. In Fig. 5, we show the relation between μ and Γ. In this case, the area under the curve represents the pattern formation area, while no pattern can be formed above it. We see that the intersection of the curve with $\Gamma_0 = 0$ is precisely the critical point obtained in [10], corresponding to $\mu_0 = 12.523205$ with $K_0 = 1.827590$. This point is shown in Fig. 4 as a black dot, and labeled in Fig. 5. The dispersion relation and the range of unstable modes where pattern formation occurs change as a function of the channel's geometric parameters, and the advective term.

In Fig. 6, we present the dispersion relation for different values of $\Gamma = -1, 0, 1$. According to Fig. 6d, the range of unstable wavenumbers $K_r = K_{max} - K_{min}$ differs for width function, for $\Gamma = -1$, $K_r = 0.326$, when $\Gamma = 1$ we obtain $K_r = 1.99$ and finally with $\Gamma = 0$ we obtain $K_r = 0.277$. The small effect cannot be neglected since the canal confinement reduces the possibility of pattern formation.

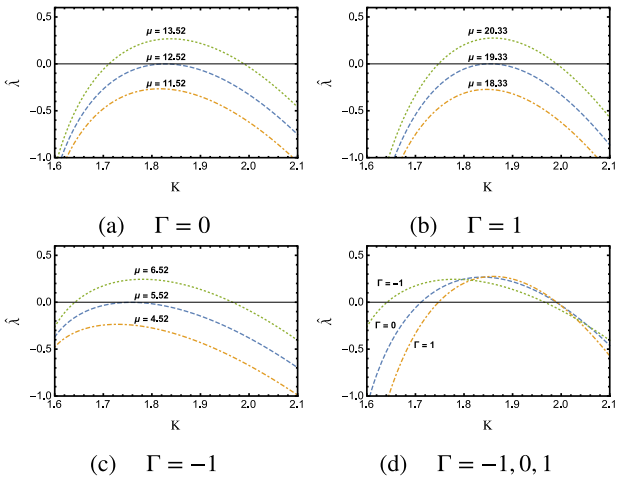

Fig. 6. Dispersion relation $\widehat{\lambda}(K)$ for prey–predator model with advection velocity v, in an exponential funnel-like channel with a generalized width function given by $w(x) = A_0 e^{-\gamma_0 x}$ for different values of the parameter Γ.

According to Eq. (33), the tuning of the parameter L_1 allows modulations of arbitrary wavelengths. When $\Gamma = 0$ for low D_N values and low population density disordered spikes can appear, probably generated by the asymmetry between birth and death processes [32], (birth events only occur adjacent to a living organism, whereas deaths occur anywhere), i.e., under reproductive fluctuations and in the presence of a weak diffusion, individuals can organize into clusters [10].

For the case $\Gamma \neq 0$, it is essential to consider that Γ is an effective advection term. In general, its value will come from the balance of the two contributions, geometric and advective. Let us consider the extreme cases to see the effects separately. When $\gamma_0 = 0$ and $v \neq 0$, it is the case of advective flow in a straight channel. The increase in Γ is due to a higher advection velocity. The negative values of Γ occur if the direction of the velocity is opposite to that of the diffusive flow, giving the additional area for pattern formation, as seen in Fig. 5. Clearly, $\Gamma = 0$ is when there is no advection. On the other hand, if $\gamma_0 \neq 0$ and $v = 0$, it is the case where the geometry of the channel induces the advective term.

For the appearance of the patterns in a channel with an exponential profile, positive values of Γ are due to the funnel-like channel shape, that is, from wide to narrow, while negative values of Γ come from the growth of the region from narrow to wide, as seen in Fig. 1, which contribute an additional area under the dispersion curve. In the latter case, the influence of geometry on the variation of the range of unstable modes that favors pattern formation is evident. Although it is the full advective term Γ which couples with the interaction rates and lengths, as analyzed previously.

4. Conclusions

The introduction of a finite-range interaction in a spatial Lotka–Volterra model allows the description of spatio-temporal dynamics characterized by regular spatial structures. We study a reaction–diffusion in an ecological system where for the reaction term, the predation strongly depends on the probability of encounter, which must take into account predators shifts in response to prey movements that means the strength of the interaction in the nonlinear term is a function of individual's proximity.

In particular, we analytically study the relationship between the interaction distance of the species and the geometric characteristics of the domain where they diffuse in the presence of an external advection current. We consider that the two-dimensional region where the reaction–diffusion process occurs is channel-shaped, i.e., when the longitudinal coordinate is much longer than the transversal one, which is reflected in a rapid equilibration in the transverse direction. Therefore, it is possible to use the one-dimensional projection method, where the equation projected along the longitudinal coordinate contains the geometric information in the channel width function and where a coordinate-dependent diffusivity may appear. The analysis was made on a long channel in the regime in which the transverse modes equilibrate much faster than the longitudinal ones, and therefore it is possible to use the Fick–Jacobs–Zwanzig operator with external force for confined diffusion.

We first made the stability analysis to study the influence of the domain's geometric characteristics in pattern formation depending on the unstable modes range given by the dispersion relation. Then we propose to calculate the Fourier transform of the reaction–diffusion–advection system where the Fick–Jacobs operator with external potential was expanded for constant diffusion coefficients.

We analyzed the instability conditions on an exponential profile channel through the effective one-dimensional projection method with different values for the shape parameter. We choose this exponential profile channel because the convolution integral gives an exact analytical expression. As a general result, we found that Γ increases the dimension of the parameter space and therefore modifies the unstable modes range. Negative values of Γ correspond to an increase of the region's area, where channels boundaries go from narrow to wide. This is also enhanced if the velocity v goes opposite to the effective flow produced by channel geometry. In this case, the appearance of patterns is favored even though the spatial solution is marked by clustering (lower L_1). Conversely, when Γ increases, the critical value increases along the curve $\mathcal{C}$ in the parameter space (K, Γ, μ) as we can see in Fig. 5. This increase may be due either to the fact that boundaries decrease from wide to narrow or because the advection velocity goes in the same direction as the geometric flow.

Generalizations to different channel shapes will be possible through numerical implementation. However, in this work, we analytically obtain that the geometric properties of the boundaries induce an effective advective term that couples with the interaction terms of the species. These results could also be extended to a three-dimensional channel with an external flow to model the dynamics of the species living in a river [29]. Then the projection method would tell us how the flow induced by geometry competes with the external flow in some specific places and how this affects species' behavior in their habitat. Finally, we point out that Brownian dynamics simulations must be carried out to verify the corresponding validity regimes. This will be done elsewhere.

CRediT authorship contribution statement

Mayra Núñez-López: Conceptualization, Methodology, Formal analysis, Investigation, Visualization, Writing – original draft, Writing – review & editing. **Guillermo Chacón-Acosta:** Conceptualization, Methodology, Formal analysis, Investigation, Visualization, Writing – original draft, Writing – review & editing.

Declaration of competing interest

The authors declare that they have no known competing financial interests or personal relationships that could have appeared to influence the work reported in this paper.

Acknowledgments

M.N.-L. acknowledges the financial support from the Asociación Mexicana de Cultura, A.C. We also thank the anonymous referees for their comments that allowed us to improve the work.

References

[1] L. Stucchi, J. Galeano, D. Vasquez, Pattern formation induced by intraspecific interactions in a predator-prey system, Phys. Rev. E 100 (2019) 062414.
[2] J.Y. Wakano, M.A. Nowak, C. Hauert, Spatial dynamics of ecological public goods, PNAS 106 (2009) 7910.
[3] H.J. Park, C.S. Gokhale, Ecological feedback on diffusion dynamics, Soc. Open Sci. 6 (2019) 181273.
[4] M.A. Nowak, R. May, Evolutionary games and spatial chaos, Nature 359 (1992) 826–829.
[5] A. Dornelas, E. Colombo, C. López, E. Hernández-García, C. Anteneodo, Landscape-induced spatial oscillations in population dynamics, Sci. Rep. 11 (2021) 3470.
[6] G. Piva, E. Colombo, C. Anteneodo, Interplay between scales in the nonlocal FKPP equation, Chaos Solitons Fractals 153 (2021) 111609.
[7] B.J. Eshel, I. Cohen, H. Levine, Cooperative self-organization of microorganisms, Adv. Phys. 49 (4) (2000) 395–554.
[8] B. Houchmandzadeh, Clustering of diffusing organisms, Phys. Rev. E 66 (2002) 052902.
[9] N.M. Shnerbj, P. Sarah, S. Lavee, Reactive glass and vegetation patterns, Phys. Rev. Lett. 90 (3) (2003) 038101.
[10] E. Brigatti, M. Oliva, M. Núñez-López, R. Oliveros-Ramos, J. Benavides, Pattern formation in a predator-prey system characterized by a spatial scale of interaction, Europhys. Lett. 88 (2009) 68002.
[11] E. Brigatti, M. Núñez-López, M. Oliva, Analysis of a spatial Lotka-Volterra model with a finite range predator-prey interaction, Eur. Phys. J. B 81 (2011) 321.
[12] F. Bartumeus, D. Alonso, J. Catalan, Self-organized spatial structures in a ratio-dependent predator-prey model, Physica A 53 (2001).
[13] P. Turchin, Complex Population Dynamics: A Theoretical/ Empirical Synthesis, Vol. 151, Princeton University Press, Princeton, 2003, p. 456.
[14] E. McGehee, E. Peacock-López, Turing patterns in a modified Lotka-Volterra model, Phys. Lett. A 342 (2005) 90–98.
[15] E. McGehee, N. Schutt, D. Vasquez, E. Peacock-López, Bifurcations, and temporal and spatial patterns of a modified Lotka-Volterra model, Int. J. Bifurcation Chaos 18 (2008) 2223.
[16] G. Sun, G. Zhang, Z. Jin, L. Li, Predator cannibalism can give rise to regular spatial pattern in a predator-prey system, Nonlinear Dynam. 58 (2009) 75–84.
[17] M. Lewis, Spatial coupling of plant and herbivore dynamics: the contribution of herbivore dispersal to transient and persistent waves of damage, Theor. Popul. Biol. 45 (1994) 277–312.
[18] R. Arditi, Y. Tyutyunov, A. Morgulis, V. Govorukhin, Directed movement of predators and the emergence of density-dependence in predator-prey models, Theor. Popul. Biol. 59 (2001) 207–221.
[19] A. Chakraborty, M. Singh, D. Lucy, P. Ridland, Predator-prey model with prey-taxis and diffusion, Math. Comput. Model. 46 (2007) 482–498.
[20] W. Sainan, W. Jinfeng, S. Junping, Dynamics and pattern formation of a diffusive predator-prey model with predator-taxis, Math. Models Methods Appl. Sci. 28 (2018) 2275–2312.
[21] J. Lee, T. Hillen, M. Lewis, Pattern formation in prey-taxis systems, J. Biol. Dyn. 3 (2009) 551–573.
[22] G. Gambino, M. Lombardo, M. Sammartino, Pattern formation driven by cross-diffusion in a 2D domain, Nonlinear Anal. RWA 14 (2013) 1755–1779.
[23] Y. Almirantis, S. Papageorgiou, Cross-diffusion effects on chemical and biological pattern formation, J. Theoret. Biol. 151 (1991) 289–311.
[24] V. Vanag, I. Epstein, Cross-diffusion and pattern formation in reaction-diffusion system, Phys. Chem. Chem. Phys. 11 (2009) 897–912.
[25] C. Varea, J. Aragón, R. Barrio, Confined Turing patterns in growing systems, Phys. Rev. E 56 (1) (1997).
[26] E. Crampin, E. Gaffney, P. Maini, Reaction and diffusion on growing domains: scenarios for robust pattern formation, Bull. Math. Biol. 61 (6) (1999) 1093–1120.
[27] A. Gabel, S.N. Majumdar, N.K. Panduranga, S. Redner, Can a lamb reach a haven before being eaten by diffusing lions? J. Stat. Mech. 05 (2012) P05011.
[28] S. Mohapatra, P.S. Mahapatra, Confined system analysis of a predator-prey minimalistic model, Sci. Rep. 9 (2019) 11258.
[29] F.M. Hilker, M.A. Lewis, Predator-prey systems in streams and rivers, Theor. Ecol. 3 (2010) 175–193.

[30] G. Chacón-Acosta, M. Núñez-López, I. Pineda, Turing instability conditions in confined systems with an effective position-dependent diffusion coefficient, J. Chem. Phys. 152 (2020) 024101.
[31] E. Hernández-García, C. López, Clustering, advection, and patterns in a model of population dynamics with neighborhood-dependent rates, Phys. Rev. E 70 (2004) 016216.
[32] W. Young, A. Roberts, G. Stuhne, Reproductive pair correlations and the clustering of organisms, Nature 412 (2001) 328–331.
[33] L. Dagdug, I. Pineda, Projection of two-dimensional diffusion in a curved midline and narrow varying width channel onto the longitudinal dimension, J. Chem. Phys. 137 (2012) 024107.
[34] R. Zwanzig, Diffusion past an entropy barrier, J. Chem. Phys. 96 (1992) 3926.
[35] D. Reguera, M. Rubí, Kinetic equations for diffusion in the presence of entropic barriers, Phys. Rev. E 64 (2001) 061106.
[36] P. Kalinay, J.K. Percus, Projection of two-dimensional diffusion in a narrow channel onto the longitudinal dimension, J. Chem. Phys. 122 (2005) 204701.
[37] P. Kalinay, J.K. Percus, Corrections to the Fick-Jacobs equation, Phys. Rev. E 74 (2006) 041203.
[38] L. Dagdug, A.A. García-Chung, G. Chacón-Acosta, On the description of Brownian particles in confinement on a non-Cartesian coordinates basis, J. Chem. Phys. 145 (2016) 074105.
[39] Y. Chávez, G. Chacón-Acosta, L. Dagdug, Unbiased diffusion of Brownian particles in a helical tube, J. Chem. Phys. 148 (2018) 214106.
[40] I. Pineda, J. Alvarez-Ramirez, L. Dagdug, Diffusion in two-dimensional conical varying width channels: Comparison of analytical and numerical results, J. Chem. Phys. 137 (2012) 174103.
[41] M. Bauer, A. Godec, R. Metzler, Diffusion of finite-size particles in two-dimensional channels with random wall configurations, Phys. Chem. Chem. Phys. 16 (2014) 6118.
[42] S. Traytak, Asymptotic solution of the diffusion equation in slender impermeable tubes of revolution. I The leading-term approximation, J. Chem. Phys. 140 (2014) 224102.
[43] A.M. Berezhkovskii, L. Dagdug, S. Bezrukov, Range of applicability of modified Fick-Jacobs equation in two dimensions, J. Chem. Phys. 143 (2015) 164102.
[44] X. Yang, C. Liu, Y. Li, F. Marchesoni, P. Hänggi, H. Zhang, Hydrodynamic and entropic effects on colloidal diffusion in corrugated channels, Proc. Natl. Acad. Sci. USA 114 (2017) 9564.
[45] P. Kalinay, Taylor dispersion in Poiseuille flow in three-dimensional tubes of varying diameter, Phys. Rev. E 102 (2020) 042606.
[46] P. Kalinay, F. Slanina, Dimensional reduction of a general advection-diffusion equation in 2D channels, J. Phys.: Condens. Matter 30 (2018) 244002.
[47] I. Pompa-García, L. Dagdug, Two-dimensional diffusion biased by a transverse gravitational force in an asymmetric channel: Reduction to an effective one-dimensional description, Phys. Rev. E 104 (2021) 044118.
[48] G. Chacón-Acosta, I. Pineda, L. Dagdug, Diffusion in narrow channels on curved manifolds, J. Chem. Phys. 139 (2013) 214115.
[49] A. Ledesma-Durán, S. Hernández-Hernández, I. Santamaría-Holek, Generalized Fick-Jacobs approach for describing adsorption-desorption kinetics in irregular pores under nonequilibrium conditions, J. Phys. Chem. C 120 (2016) 7810.
[50] A. Ziepke, S. Martens, H. Engel, Wave propagation in spatially modulated tubes, J. Chem. Phys. 145 (2016) 094108.